



**Progress toward defining the molecular identities of  
neocortical neurons**

Journal:	<i>Journal of Cell Identity</i>
Manuscript ID	CELLID-2021-0003.R1
Manuscript Type:	Review
Date Submitted by the Author:	27-Oct-2021
Complete List of Authors:	Deleanu, Roxana; Medical University of Innsbruck, Institute for Neuroscience
Keywords:	cortical neurons, taxonomy, single cell transcriptomics, single cell multiomics, cortical neurogenesis

SCHOLARONE™  
Manuscripts

1  
2  
3  
4  
5  
6  
7  
8  
9  
10  
11  
12  
13  
14  
15  
16  
17  
18  
19  
20  
21  
22  
23  
24  
25  
26  
27  
28  
29  
30  
31  
32  
33  
34  
35  
36  
37  
38  
39  
40  
41  
42  
43  
44  
45  
46  
47  
48  
49  
50  
51  
52  
53  
54  
55  
56  
57  
58  
59  
60

**Progress toward defining the molecular identities of neocortical neurons**

Roxana Deleanu

**Abstract**

The neurons that make up the human cerebral cortex are responsible for a wide array of higher cognitive, social-emotional, sensory and motor functions. These very complex functions are supported by a rich diversity of excitatory and inhibitory neurons, each of which has its own developmental pathway, and is specifically assembled into highly complex cortical circuits with powerful computational capacities. Recent studies using single-cell transcriptomics, single-cell electrophysiological recordings, and morphological reconstruction have begun to reveal surprising levels of neuronal diversity in mammals, defined by distinctive transcriptomic signatures, morphological, and physiological phenotypes. While most of the available data rely on studies performed on mouse neocortex, several recent findings in the human neocortex point to both conserved molecular profiles, and human-specific differences. Herein, the main milestones in the classification of neocortical neurons are discussed, beginning with the “classical” combination of a few class-specific marker expression and cell morphologies, and progressing to their origin and recent multiplex profiling. While single-cell and single-nucleus RNA sequencing data provide a huge progress in neuronal taxonomy, the boundaries between subclasses can be defined and validated only in combination with morphological and electrophysiological features.

**Key words:** cortical neurons, taxonomy, single-cell transcriptomics

**1. Introduction**

The cerebral cortex is the most developed part of the human brain and is recognized as the most complex structure in the human body, with sensory and motor functions but also with higher level cognitive and social-emotional functions (DeFelipe, 2011). Deciphering its composition, functions and dysfunctions continues to be one of the

main concerns in neuroscience, medicine, and psychology. Neuroscience research, which began more than 120 years ago with the studies of Ramon y Cajal on the morphology diversity of neurons in the cerebral cortex, has recently reached an exponentially growing phase, with several international large-scale efforts devoted to the analysis and understanding of brain composition, development, and functions. Single-cell high throughput approaches provide unprecedented details on cellular diversity. Major efforts are now directed towards generating a complete description of cell types based on molecular criteria, addressing the neocortex (Allen Institute for Brain Science, [www.allenbrain.org](http://www.allenbrain.org)), the whole brain (the National Institutes of Health (NIH) BRAIN Initiative Cell Census Network (BICCN), [braininitiative.nih.gov](http://braininitiative.nih.gov)), and even the whole body (the Human Cell Atlas, [www.humancellatlas.org](http://www.humancellatlas.org)) (Bakken *et al.*, 2016; Ecker *et al.*, 2017; Regev *et al.*, 2017; Yuste *et al.*, 2020).

Nearly 100 billion neurons are found in the human brain, with 16-20 billion in the cerebral cortex, as well as three to five times more glial and non-neural cells (Azevedo *et al.*, 2009; Lent *et al.*, 2012). Neurons are generally very heterogeneous; they differ in terms of biochemical and electrical properties, morphologies and connections (Eyal *et al.*, 2016), although some of them share common features. The classification of neurons in the cerebral cortex is very challenging, and no consensus has yet been reached. Their intrinsic properties, such as neurochemical profile (neurotransmitters, associated neuropeptides, receptors), location, morphology (dendritic and axonal morphologies), and connectivity (projections to and from other neurons), as well as electrophysiological behavior, can be used to classify them. Traditionally, cell type diversity in a particular brain region was determined by cross-referencing neuronal morphology with the expression of a few molecular markers and the type of response to electrical stimuli. Many morphological and physiological neuronal features, as well as the molecular expression of a certain cell subtype, have been described for several species, including humans, and both conserved patterns and variations between species have been documented (Hill and Walsh, 2005; Hawrylycz *et al.*, 2015; Eyal *et al.*, 2016; Boldog *et al.*, 2018). Nevertheless, understanding the cellular composition of the human cortex and its level of conservation presents many challenges.

Recently, a set of high-throughput techniques and bioinformatics tools has vastly expanded the scope of inquiry and allowed for significant advances in defining cellular

1  
2  
3  
4  
5  
6  
7  
8  
9  
10  
11  
12  
13  
14  
15  
16  
17  
18  
19  
20  
21  
22  
23  
24  
25  
26  
27  
28  
29  
30  
31  
32  
33  
34  
35  
36  
37  
38  
39  
40  
41  
42  
43  
44  
45  
46  
47  
48  
49  
50  
51  
52  
53  
54  
55  
56  
57  
58  
59  
60

identities, including in the cerebral cortex. Single-cell high-throughput technologies, including RNA deep sequencing, epigenomics, proteomics, and metabolomics, provide a far more comprehensive biological understanding than bulk sequencing and proteomics analyses in the past. Single cells or nuclei provide the scale for an unbiased survey on molecular expression (Bakken *et al.*, 2018). In addition, powerful multiplex single-cell technologies employing novel biosensors enable further refinement of the subtypes defined at the transcriptional level by addressing their electrophysiological and metabolic states in parallel. Importantly, these tools have overcome some of the previous difficulties associated with the scarcity of human brain tissue and have demonstrated that these modern approaches can be applied to relatively small human postmortem and neurosurgical tissue samples (Krishnaswami *et al.*, 2016; Lake *et al.*, 2017)

Several newly released methodologies, such as spatial reconstruction (Gouwens *et al.*, 2020) and spatial transcriptomics (Battich, Stoeger and Pelkmans, 2013; Moffitt *et al.*, 2016; Lein, Borm and Linnarsson, 2017; Wang *et al.*, 2018; La Manno *et al.*, 2021; Langseth *et al.*, 2021) provide important information needed to interpret the meaning of single-cell multiomics results and enrich the picture by addressing each single cell in its normal tissue context. Multiple single-cell analyses and spatial reconstructions are now combined to better characterize the cells that make up the nervous system (Yuste *et al.*, 2020). Most of these methods have been tested on the rodent brain (Cadwell *et al.*, 2016; Tasic *et al.*, 2017; Gouwens *et al.*, 2020; La Manno *et al.*, 2021), the most commonly used model in neuroscience, but a growing number of studies and databases are adding results from human brain tissue (Darmanis *et al.*, 2015; Ecker *et al.*, 2017; Regev *et al.*, 2017; Lake *et al.*, 2018; Hodge *et al.*, 2019), including the cerebral cortex (Langseth *et al.*, 2021).

This review aims to combine “classical” and recent “omics” knowledge about neuronal diversity, organization, and development in the mouse cerebral cortex with the knowledge from the human cerebral cortex.

**2. From anatomy to the morphological organization of the mammalian cerebral cortex**

The adult human cerebral cortex, which is the largest part of the brain, has a highly folded structure with many grooves and gyri. This anatomical aspect defines the gyrencephalic brain, which is found in primates as well as dolphins, elephants, pigs, marmosets, dogs, cats, and even ferrets (Glezer, Bittencourt and Rivest, 2009; DeFelipe, 2011). Even though their brains are lissencephalic, with a smooth, unfolded cortical surface and a far lower volume than gyrencephalic brains, rodents are the most utilized model organisms in brain medical research. Remarkably however, the ratio of ~1:1000 is maintained between mouse and human for both brain volume and neuronal number in the cerebral cortex (Herculano-Houzel, Mota and Lent, 2006). Furthermore, basic architecture and cellular composition of the brain appear to be fairly similar between mammals. The conserved anatomical, morphological and functional features of the mammalian cerebral cortex have been extensively studied in recent decades (DeFelipe, 2011; Lui, Hansen and Kriegstein, 2011; Molnár and Clowry, 2012; Greig *et al.*, 2013; Cadwell *et al.*, 2019).

The cerebral cortex contains a network of neurons with cell bodies arranged in cytoarchitectonic structures named layers. The neocortex (or isocortex, referred to as cortex in many papers and hereafter) is the most extended region of the cerebral cortex, with six layers labeled layer I-VI or 1-6 (L1-L6, also hereafter) (**Fig 1**). L1 faces the pia mater, while L6 faces the white matter of the cerebrum. The upper layers range from L1 to L4, with L4 being the (internal) granular layer and L2 and L3 being supragranular layers. L5 and L6 are the deep (or infragranular) layers. The number of neurons and their distribution in each layer vary in different anatomical areas and sub-areas of the mammalian cortex (such as motor, sensory, auditory, parietal or visual) (Amunts and Zilles, 2015; García-Cabezas, Hacker and Zikopoulos, 2020).

The cortical thickness and cell density of each layer are widely used as markers for the area characterization, both *in vivo* and *ex vivo*. The thickness of the entire cortex is mostly proportional to the density of neurons. The cortical and laminar thickness in different human brain regions were measured in histological brain sections, such as those provided by Brodmann and von Economo (Amunts and Zilles, 2015; García-Cabezas, Hacker and Zikopoulos, 2020) or in whole-brains, such as those provided by the *BigBrain* Project (Amunts and Zilles, 2015; García-Cabezas, Hacker and Zikopoulos, 2020; Wagstyl *et al.*, 2020). Cortical thickness ranges from 1.8 mm in the

1  
2  
3  
4  
5  
6  
7  
8  
9  
10  
11  
12  
13  
14  
15  
16  
17  
18  
19  
20  
21  
22  
23  
24  
25  
26  
27  
28  
29  
30  
31  
32  
33  
34  
35  
36  
37  
38  
39  
40  
41  
42  
43  
44  
45  
46  
47  
48  
49  
50  
51  
52  
53  
54  
55  
56  
57  
58  
59  
60

occipital cortex around the calcarine sulcus to 4.5 mm in the precentral gyrus, which contains the primary motor cortex. The thickness of the human cortex ranges around 2-3 mm in most regions,, whereas in mouse it varies between 1 and 2 mm (*Brain Map* - *brain-map.org*, no date). The motor cortex is especially thick in both species. At the laminar level, L3, 5, and 6 contribute the most to overall thickness, while L4 is highly variable and defines several density-related architectural types such as granular (koniocortex), agranular, dysgranular and eulaminate I-III (García-Cabezas, Hacker and Zikopoulos, 2020). The most investigated cortical area, both *in vivo* and *ex vivo*, is the mouse visual cortex area V1 (Froudarakis *et al.*, 2019), where it is estimated that a cortical surface of 1 mm<sup>2</sup> includes roughly 10<sup>5</sup> neurons in all layers (in ~ 1mm<sup>3</sup>) (*Brain Map* - *brain-map.org*, no date).

3. The “classical” characterization of cortical neurons: morphology, projections, neurotransmitters, neuropeptides and electrical responses

Neurons from all cortical areas are divided into two major categories: **excitatory neurons** and **inhibitory neurons** (**Fig. 1**). Excitatory neurons, also known as principal cells, account for about 80% of cortical neurons (Molnár and Clowry, 2012).

Cell body size can vary significantly for both categories of cortical neurons, but the shape and orientation of their projections are the most prominent morphological characteristics. Morphologically, excitatory neurons present mainly “spiny” aspects of their projections, while inhibitory neurons present “aspiny” (or “smooth”) aspects. While most excitatory neurons have pyramidal somas and elaborated dendrites, some L4 neurons exhibit “star pyramid” or “spiny stellate” morphologies (Staiger *et al.*, 2004). Inhibitory neurons come in a wide variety of shapes and sizes: basket, bipolar, bouquet, chandelier, canopy, rosehip (Boldog *et al.*, 2018), etc., some of which have specific names, such as Martinotti cells or non-Martinotti cells (Lim *et al.*, 2018; Mihaljević *et al.*, 2019).

The most widely used “classical” classification system for excitatory neurons in the cortex using **glutamate** for synaptic communication is based on their anatomical connections, and includes three primary (first-order) classes (*Exc I-III*) (Harris and Shepherd, 2015; Baker *et al.*, 2018) (**Figs. 1 and 2**). The first class (*Exc I*) comprises the cortico-thalamic (CT) neurons, which are predominantly located within L6 and

project to the thalamus. The second class (*Exc II*) comprises the cortico-fugal (CF) neurons, which are found mainly within L5 and extend axons toward the brainstem and spinal cord, with some of them forming the pyramidal tract (PT). The third and most heterogeneous class (*Exc III*) is represented by the intra-telencephalic (IT) projection neurons, located in L2-6 and extending axons toward targets in the contralateral and ipsilateral cortex, striatum, nucleus accumbens, septum, and nuclei of amygdala. Several subclasses are defined by subsets of neurons within the primary classes that project to multiple targets. For example, several IT neurons in L4 with distinct morphologies (e.g., spiny stellate and star pyramidal) have local synaptic outputs and thalamic synaptic inputs. All cortical regions contain neurons from each of the three primary classes, but their percentage and specific targets/subclasses vary depending on the area in which they reside.

The most commonly used “classical” classification for cortical **inhibitory neurons**, all of which use  **$\gamma$ -aminobutyric acid** (GABA) for synaptic communication, comprises three primary (first-order) classes, *Inh I-III* (**Figs 1 and 2**). Neurons from the first two classes (*Inh I* and *Inh II*) co-express the neuropeptides **parvalbumin** (PV/Pv or Pvalb/PVALB, as noted for mouse/human) and **somatostatin** (Som/SOM or Sst/SST), respectively (the second abbreviations will be used hereafter), while the third class (*Inh III*) is more heterogeneous. The serotonin receptor **5Ht3ar** is expressed in all mouse *Inh III* neurons (Lee *et al.*, 2015; Lim *et al.*, 2018), but not in human *Inh III* neurons (Hodge *et al.*, 2019). Several subtypes from each inhibitory class populate the mouse and human cortex, with a relatively consistent molecular expression and morphology (Xu, Roby and Callaway, 2010; Hawrylycz *et al.*, 2015; Tremblay, Lee and Rudy, 2016; Lim *et al.*, 2018; Mihaljević *et al.*, 2019).

GABAergic Pvalb+ neurons form the most consistent class (*Inh I*), accounting for roughly 40% of inhibitory neurons and divided into three subclasses of interneurons, each corresponding to one of three specific morphologies: basket, chandelier and translaminar cells (**Fig. 2**). Basket cells are the most abundant subtype in the *Inh I* class and in cortex and may be found from L2 to L6 in all cortical regions. They form synapses with the cell bodies and proximal dendrites of pyramidal cells and other interneurons. Chandelier and translaminar cells are less common subclasses with a



1  
2  
3  
4  
5  
6  
7  
8  
9  
10  
11  
12  
13  
14  
15  
16  
17  
18  
19  
20  
21  
22  
23  
24  
25  
26  
27  
28  
29  
30  
31  
32  
33  
34  
35  
36  
37  
38  
39  
40  
41  
42  
43  
44  
45  
46  
47  
48  
49  
50  
51  
52  
53  
54  
55  
56  
57  
58  
59  
60

heterogeneous regional distribution. Chandelier cells form synapses with the initial segment of the axons from pyramidal cells (Woodruff, Anderson and Yuste, 2010). Translaminar neurons have cell bodies residing in deep cortical layers and axons with arborizations throughout all layers (Bortone, Olsen and Scanziani, 2014).

GABAergic Sst+ cells (*Inh II*), comprising around 30% of cortical inhibitory neurons, are predominantly interneurons and only a few are projection neurons (**Fig. 2**). Sst+ interneurons have two morphological types: Martinotti cells and non-Martinotti cells. Martinotti cells are the most consistent subclass, with ascending axons that arborize profusely in L1 (Wang *et al.*, 2004). They are found throughout L2-6, particularly abundant in L5-6 and frequently co-expressing calbindin (Cb/CB or Calb1/CALB1) or calretinin (Cr/CR or Calb2/CALB2). Non-Martinotti cells are also found throughout L2-6, where they primarily target the Pvalb+ basket cells. Sst+ projection neurons constitute a rare subtype found mostly in L6 and the adjacent white matter and they typically co-express nitric oxide synthase (Nos/NOS).

GABAergic cortical neurons of the third class (*Inh III*), which make up about 30% of cortical inhibitory neurons, have a wide range of morphologies and co-expressed peptides (**Fig. 2**). The interneurons that express vasoactive intestinal peptide (Vip/VIP) form the largest *Inh III* subclass in both mice and humans. They preferentially target the Sst+ and Pvalb+ interneurons and produce a disinhibitory effect. Bipolar cells with vertically oriented axons, highly enriched in L2, 3 and 4, and often co-expressing Calb2 are the most recognizable Vip+ interneurons. They are especially enriched in the human cortex (13% vs. 4% in mouse), half of them residing in frontal associative areas (Hladnik *et al.*, 2014). Basket cells that co-express the neuropeptide cholecystokinin (Cck/CCK) and are particularly abundant in the upper layers are another Vip+ subtype. Some Cck+ basket cells lack Vip and are enriched in L5-6, forming synapses with cell bodies of pyramidal cells and other interneurons. Neurogliaform cells, single bouquet cells, and multipolar cells are examples from another subclass that lacks Vip expression. Neurogliaform cells and single bouquet cells co-express reelin (Reln/RELN) and are the most abundant types of interneurons in L1, although neurogliaform cells are sparsely distributed throughout the other layers. Neurogliaform cells form a very dense and characteristic projection arbor in L1, while single bouquet cell projections extend to deeper layers. Multipolar interneurons co-express the



neuropeptide Y (Npy/NPY) and are particularly abundant along the L1-L2 border (Raghanti *et al.*, 2013). Interstitial neurons residing in the white matter and extending axons to deep layers and subcortical neurons form another, less well described subclass. Many of these cells express Meis/MEIS and share Pvalb or Sst expression (Kostović, Judaš and Sedmak, 2011).

Both excitatory and inhibitory neurons in the cortex process and encode information by generating action potentials in a wide range of shapes, frequencies and patterns. Whole-cell patch clamp recordings, using a variety of stimulus protocols, provide basic information about cell firing properties, which can be used to assess intrinsic neuronal properties. Several studies have addressed electrical recordings *in vivo*, *ex vivo* (in slice cultures or dissociated neurons), and *in vitro*, in primary cultures. Three distinct electrophysiological behaviors were observed in cortical neurons: regular-spiking, bursting, and fast-spiking. Mihaljević *et al.* found that mature glutamatergic neurons elicit fast-spiking profiles with high firing frequencies, whereas mature GABAergic neurons elicit a multitude of profiles and frequencies, ranging from spiking (fast, regular, and irregular) to continuous bursting (Mihaljević *et al.*, 2019). Again, the electrophysiological properties of cortical neurons do not significantly differ between cortical areas (Tremblay, Lee and Rudy, 2016; Lim *et al.*, 2018; Mihaljević *et al.*, 2019).

#### 4. Genesis of cortical neuron classes and subclasses

Optimal classification of cortical neuronal subtypes should include their developmental and maturation paths. The development of the nervous system entails the precise temporal and spatial generation of each cell type. The high diversity of cortical neurons requires the formation of a wide range of progenitor cell types. Progenitor type and location, the migration pathways newborn neurons undertake to reach their final destination in the mature cortex are all elements which factor in the creation of neurons (**Fig. 3**). Several experiments combining *in vivo* lineage analysis with genetic loss-of-function and gain-of-function identified key molecular players in the development of the rodent brain. Combined with descriptive research on human embryos, these experiments revealed conserved stages during mammalian brain development, which include neural induction, patterning/proliferation, neurogenesis, gliogenesis, and functional maturation (Finlay and Darlington, 1995; Shen *et al.*, 2006; Wonders and

1  
2  
3  
4  
5  
6  
7  
8  
9  
10  
11  
12  
13  
14  
15  
16  
17  
18  
19  
20  
21  
22  
23  
24  
25  
26  
27  
28  
29  
30  
31  
32  
33  
34  
35  
36  
37  
38  
39  
40  
41  
42  
43  
44  
45  
46  
47  
48  
49  
50  
51  
52  
53  
54  
55  
56  
57  
58  
59  
60

Anderson, 2006; Zhao *et al.*, 2008; Lodato and Arlotta, 2015; Turrero García and Harwell, 2017; Cadwell *et al.*, 2019) .

Brain development starts with neural induction, when cellular pluripotency in the early embryo entering the gastrula stage is gradually lost in the anterior midline ectoderm. The newly formed neuroectoderm containing neuroepithelial stem cells (NESCs) organizes the neural plate (NP), which further extends and creates neural folds; the gradual dorso-median fusion of the neural folds leads to the formation of the neural tube (NT), a process called neurulation (and related to the neurula stage). NESCs are first detected in mice around embryonic day (e) 7 and in humans around gestation week (GW) 4. After several symmetric divisions, around e9/GW 5-6, NESCs begin a transition into more elongated, radial-oriented cells called radial glial cells (RGCs), in which the basal and apical processes remain in contact with the lumen, and the pial surface of the NT, respectively. RGC somas are found in the ventricular zone (VZ) of the NT wall until around e11, when they undergo symmetric proliferative divisions, resulting in the expansion of the progenitor pool. In addition, NT cells acquire different identities in the anterior-posterior (A-P) and dorsal-ventral (D-V) axes due to the gradients of morphogens produced by organizer centers. This process is called patterning and takes place in a temporal and spatial order, determining the transcriptional code and the identity of neural cells in a particular domain. The anatomical and molecular definition of the main regions/vesicles in the developing brain are determined by patterning and proliferation. A-P patterning starts in the head region with the forebrain (prosencephalon), which further divides into telencephalon and diencephalon. In the developing telencephalic vesicle, D-V patterning creates two main regions: dorsal telencephalon or pallium, and ventral telencephalon or subpallium.

In parallel with the patterning, progenitor cells situated in different domains proliferate at varying rates in response to local mitogens (Turrero García and Harwell, 2017; Lim *et al.*, 2018). The pallium forms three longitudinal domains: dorsal, medial, and lateral. The dorsal pallium further develops into the neocortex, the medial pallium into the hippocampus (archicortex), and the lateral pallium into the olfactory cortex and some limbic areas (paleocortex). The cells in subpallium proliferate more intensely and form several domains defined in D-V and A-P axes, called lateral, medial, and caudal

ganglionic eminences (LGE, MGE, and CGE, respectively), preoptic region, and septum. Each of these domains has its own set of subdomains. MGE is broadly divided into dorsal (dMGE), intermediate (iMGE), and caudoventral (cvMGE) regions. The preoptic region consists of two adjacent domains: preoptic area (POA) and preoptic-hypothalamic (POH) border domain (Turrero García and Harwell, 2017).

Telencephalic neurogenesis takes place in a tightly controlled temporal and spatial order from e11 to e18 (corresponding to ~GW5-12 in humans). RGCs can produce neurons directly through asymmetrical division, or indirectly through transit-amplifying progenitors, such as intermediate progenitor cells (IPCs) (Kriegstein, Noctor and Martínez-Cerdeño, 2006). IPCs generate neurons either directly or after a series of symmetric divisions. Somas of the neurogenic precursors (RGCs or IPCs) are located in the VZ or in the subventricular zone (SVZ), while newborn neurons use the processes of RGCs as scaffolds to migrate superficially toward the marginal zone (MZ) of the NT. After neurogenesis is complete in rodents, or in a late stage in humans, the RGCs proceed to gliogenesis, producing astrocytes, ependymal cells and oligodendrocytes.

Progenitors in the pallium give rise to all glutamatergic neurons in the telencephalon, whereas progenitors in the subpallium give rise to GABAergic neurons in the cortex (**Fig. 3**) and GABAergic and cholinergic neurons in the ventral telencephalon (forming the adult basal ganglia, centromedial extended amygdala, septum, and preoptic region) (Turrero García and Harwell, 2017).

Cajal-Retzius cells (CRCs) are the earliest neurons born in the pallium, which accumulate in the MZ and form the preplate. When the next generation of neurons arrives, the preplate organizes into two regions: a superficial one, where CRCs accumulate and L1 is formed, and a deeper one, called the subplate, which contains another transitory population of neurons. Newly coming neurons are settled between these two zones and the region called the cortical plate begins to develop. The newborn neurons that make their way from the SVZ to the cortical plate adopt a position corresponding to their age, mainly in an inside-first, outside-last (inside-out) order. The layer location of a cortical neuron is tightly linked to the timing of its production. This temporal patterning results in the sequential generation of layer-

1  
2  
3  
4  
5  
6  
7  
8  
9  
10  
11  
12  
13  
14  
15  
16  
17  
18  
19  
20  
21  
22  
23  
24  
25  
26  
27  
28  
29  
30  
31  
32  
33  
34  
35  
36  
37  
38  
39  
40  
41  
42  
43  
44  
45  
46  
47  
48  
49  
50  
51  
52  
53  
54  
55  
56  
57  
58  
59  
60

specific types of cortical neurons and is a fundamental process of neuronal diversification (Hébert and Fishell, 2008; Cadwell *et al.*, 2019). CT neurons develop from the first neurons migrating from the SVZ to the newly formed cortical plate. The next generation of neurons mostly matures into CF neurons. The latest born neurons migrate past the earlier born neurons and mature into IT neurons (Kwan, Šestan and Anton, 2012; Cadwell *et al.*, 2019). The recently described outer SVZ (oSVZ) in the human fetal cortex is enriched in a cell type known as outer radial glial cell (oRGC), which has lost contact with the NT lumen and proliferates during the longer-lasting human neurogenesis, producing mainly the large diversity of IT neurons in the human cortex (Hansen *et al.*, 2010; Betizeau *et al.*, 2013; Bakken *et al.*, 2016).

Subpallium neurons migrate dorsally to the cortex or remain in the ventral telencephalon. For the specification of various neuronal subtypes here, there is once again a temporal control. In general, projection neurons (GABAergic or cholinergic) are born first, followed by interneurons (GABAergic or cholinergic) (Turrero García and Harwell, 2017). Both mouse and human cortical GABAergic interneurons are derived primarily from three subpallial progenitor regions: MGE (the majority), CGE, and preoptic regions (Wonders and Anderson, 2006; Hansen *et al.*, 2013; Lim *et al.*, 2018). MGE and POA generate virtually all the interneurons in the *Inh I* (Pvalb+) and *Inh I* (Sst+) classes. The progenitors in the dMGE have a strong bias toward the development of Sst+ neurons (Martinotti cells, non-Martinotti cells, and long-range neurons), whereas those in the iMGE produce both Pvalb+ and Sst+ interneurons, and those in the vMGE produce a larger fraction of Pvalb+ interneurons (basket, chandelier and translaminar cells). CGE and preoptic region progenitors produce mainly class III GABAergic neurons: basket, bipolar, and single bouquet cells in CGE, neurogliaform, multipolar Npy+ interneurons most likely in POH, and interstitial cells most likely in POA. Some interstitial and neurogliaform GABAergic subpopulations could have pallial origins (Kostović, Judaš and Sedmak, 2011; Lim *et al.*, 2018).

The GABAergic interneurons generated in the MGE, CGE, and preoptic regions use essentially the same cellular mechanisms to translocate to the developing cortex in a protracted period of migration, *via* two large migratory streams: a superficial route through the MZ and a deep route through the SVZ. These neurons have an immature phenotype when reaching the pallium and their maturation continues long after birth.

The future Sst+ Martinotti and Pvalb+ translaminal interneurons migrate preferentially through the MZ route, while Sst+ non-Martinotti cells use the SVZ route. Several lines of evidence suggest that interneurons adopt a laminar distribution in response to cues provided by pyramidal cells. Similar to pyramidal cells, they follow an “inside-out” sequence that correlates with their birthdates: earlier formed Sst+ interneurons are more abundant in deep layers, while recently generated Pvalb+ chandelier cells are located mainly in the superficial layer (Lim *et al.*, 2018).

## 5. RNA profiling of mouse and human cortical neurons

RNA sequencing (RNA-seq) is a technique that uses high throughput, next-generation sequencing approaches to analyze the cellular or subcellular transcriptome in order to reveal the presence and quantity of RNA in a biological sample at a given moment. Recent advances in RNA-seq include single cell and single nucleus RNA-seq (scRNA-seq and snRNA-seq, respectively) (Tang *et al.*, 2009; Krishnaswami *et al.*, 2016; Bakken *et al.*, 2017), *in situ* sequencing of fixed tissue, called spatial transcriptomics (Lein, Borm and Linnarsson, 2017), as well as novel platforms for integrating single cell and spatial transcriptomics data (Butler *et al.*, 2018).

Since the first single cell experiment published in 2009 (Tang *et al.*, 2009), scRNA-seq has become the quasi-standard method for profiling heterogeneous cell populations. The recent advent of high-throughput microfluidic systems with droplet-based profiling techniques has further advanced the precision of sc/sn RNA-seq profiling (Habib *et al.*, 2017). Unlike bulk RNA sequencing, which interrogates average gene expression in cell populations that are in most cases heterogeneous (Lein *et al.*, 2007), scRNA-seq can elucidate the heterogeneity and allow for cell-type specific transcriptome profiling. Initially limited to only a few hundred cells per experiment, due to advances in experimental technologies, more than 1 million single cell transcriptomes can now be profiled (Habib *et al.*, 2017).

In order to analyze complex sets of single cell data, robust computational methodologies are required. For single cell clustering and cell type annotation, two computational approaches, unsupervised and supervised, are routinely used, each

1  
2  
3  
4  
5  
6  
7  
8  
9  
10  
11  
12  
13  
14  
15  
16  
17  
18  
19  
20  
21  
22  
23  
24  
25  
26  
27  
28  
29  
30  
31  
32  
33  
34  
35  
36  
37  
38  
39  
40  
41  
42  
43  
44  
45  
46  
47  
48  
49  
50  
51  
52  
53  
54  
55  
56  
57  
58  
59  
60

with its own set of advantages and limitations (Bakken *et al.*, 2017). The unsupervised approach uses clustering followed by cluster annotation using marker genes (Kiselev, Andrews and Hemberg, 2019). Clusters identified in an unsupervised manner are typically annotated to cell types based on differentially expressed genes. The supervised approach uses a reference panel of labelled transcriptomes to guide both clustering (Li *et al.*, 2017) and cell type identification (Abdelaal *et al.*, 2019). Therefore, they can lead to different but often complementary clustering results. Hence, a consensus approach leveraging the merits of both clustering paradigms could result in a more accurate clustering and cell type annotation (Ranjan *et al.*, 2021).

Several transcriptomic studies performed with single cells or nuclei from cortex tissue both rodent (Zeisel *et al.*, 2015; Bakken *et al.*, 2016; Johnson and Walsh, 2017; Tasic *et al.*, 2017; Gouwens *et al.*, 2020) and human (Kang *et al.*, 2011; Darmanis *et al.*, 2015; Lake *et al.*, 2016, 2018; Boldog *et al.*, 2018; Hodge *et al.*, 2019; Velmeshev *et al.*, 2019) have already provided many biological insights. The clustering of cortical cell types was obtained using unsupervised and supervised methods, or a combination of them. Each cluster was given “unique markers”, which are genes that are expressed only in that cell type, as well as “combinatorial markers”, which are differentially expressed genes not restricted to a single cell type. In several supervised approaches, NeuN and Snap25 were used as pan-neuronal markers, Slc17a7 and Neurod6 as markers for excitatory neurons, and Gad1 and Gad2 as markers for inhibitory neurons. The mRNA expression of major known neuronal marker genes: *Snap25*, *Gad1* and *Slc17a7*, for example, was used to characterize neuronal clusters in the mouse primary visual cortex (Tasic *et al.*, 2016; Gouwens *et al.*, 2020). Further sequential cell annotations identified 49 transcriptomic cell types (Tasic *et al.*, 2016), including 23 transcriptomic cell types in the GABAergic neuronal cluster (*Snap25*<sup>+</sup>, *Slc17a7*<sup>-</sup>, *Gad1*<sup>+</sup>) and 19 transcriptomic cell types in the glutamatergic neuronal cluster (*Snap25*<sup>+</sup>, *Slc17a7*<sup>+</sup>, *Gad1*<sup>-</sup>). Within this genome-wide dataset, glutamate and GABA receptors were shown to be widely expressed in neurons, while neuropeptide genes were usually selectively expressed in one or a few GABAergic cell types (Tasic *et al.*, 2016).

Transcriptomic data were integrated into constellation diagrams that summarize the identity, marker genes and putative location of glutamatergic and GABAergic cell types



1  
2  
3 along the pia mater to white matter axis (**Figs. 4A** and **5A**). Within these diagrams,  
4 each transcriptomic cell type is represented by a disc, whose surface area  
5 corresponds to the number of core cells in the dataset belonging to that type.  
6  
7 Intermediate situated cells are represented by lines connecting the discs; line  
8 thickness is proportional to the number of intermediate cells. This type of  
9 representation depicts the overall phenotypic landscape of cortical cell types as a  
10 combination of continuity and discreteness: the presence of a large number of  
11 intermediate cells between a particular pair of core types suggests a phenotypic  
12 continuum, while the absence of intermediate cells connecting one type to another  
13 indicates its more discrete nature.  
14  
15  
16  
17  
18  
19  
20

21  
22 Based on layer-specific expression of marker genes and layer-enriching dissections,  
23 computational analysis has identified six major classes of transcriptomic types for  
24 excitatory neuronal clusters (**Fig. 4A**): L2/3, L4, L5a, L5b, L6a, and L6b. Four  
25 transcriptomic cell types were identified for the L6a types and two for the L6b types.  
26 Two highly related L6a types (L6a-Sla and L6a-Mgp) express the marker *Foxp2*, while  
27 the other two (L6a-Syt17 and L6a-Car12) do not. The two L6b types (L6b-Serpinb11  
28 and L6b-Rgs12) both express *Ctgf*, as well as several other previously reported L6b  
29 markers (e.g., *Trh*, *Tnmd*, *Mup*). There were eight different transcriptomic types  
30 identified within the L5 types. Four of them express the L5a marker *Deptor* (L5a-  
31 *Hsd11b1*, L5a-*Tcerg1l*, L5a-*Batf3*, and L5a-*Pde1c*), while three express the L5b  
32 marker *Bcl6* (L5b-*Cdh13*, L5b-*Tph2*, and L5b-*Chrna6*, Fig 3b). Based on gene  
33 expression and the small number of intermediate cells between them and other L5  
34 types, one of the L5b types (L5b-*Chrna6*), along with the L5-*Ucma* type, appear to be  
35 the most distinct among L5 types. Within L4, the three subdivisions (L4-*Ctxn3*, L4-  
36 *Scnn1a* and L4-*Arf5*) present high gene expression similarity and a large number of  
37 intermediate cells. L2-*Ngf* and L2/3-*Ptgs2* were identified as subdivisions of L2/3.  
38  
39  
40  
41  
42  
43  
44  
45  
46  
47  
48  
49

50 Computational analysis identified 17 cell types for inhibitory neuronal clusters (**Fig.**  
51 **5A**), of which seven cell types express *Pvalb*, six cell types express *Sst*, five cell types  
52 express *Vip*, and two cell types express neuron derived neurotrophic factor (*Ndnf*).  
53 The other three GABAergic types express synuclein gamma (*Sncg*), interferon gamma  
54 induced GTPase (*Igtp*), and SMAD family member 3 (*Smad3*). Several known markers  
55  
56  
57  
58  
59  
60



1  
2  
3  
4  
5  
6  
7  
8  
9  
10  
11  
12  
13  
14  
15  
16  
17  
18  
19  
20  
21  
22  
23  
24  
25  
26  
27  
28  
29  
30  
31  
32  
33  
34  
35  
36  
37  
38  
39  
40  
41  
42  
43  
44  
45  
46  
47  
48  
49  
50  
51  
52  
53  
54  
55  
56  
57  
58  
59  
60

such as Calb1, Calb2, Cck, Htr3a, Nos1, Npy, Reln are expressed in different subtypes.

All the Pvalb cell types are highly interconnected in the constellation diagrams. Some cell types are preferentially located in the upper layers (Pvalb-Tpbpg, Pvalb-Tacr3, Pvalb-Cpne5) or the deep layers (Pvalb-Gpx3 and PvalbRspo2). Five Sst cell types are enriched in the deep layers, whereas one (Sst-Cbln4) is prevalent in the upper cortical layers. Cell types expressing Vip co-express Calb2 and several other markers, such as choline acetyltransferase (Chat). Vip-Gpc3 type is located in the deep layers, while Vip-Chat type is located in the upper layers.

Transcriptional analysis of nuclei isolated from human cortex samples (obtained either postmortem or during surgery, in which NeuN positive neuronal nuclei were selected) (Hodge *et al.*, 2019) followed the same computational analysis as in the previously profiled mouse cortical cells (Tasic *et al.*, 2016). The analysis revealed 24 clusters representing different types of excitatory neurons (*versus* 19 in mouse) (**Fig. 4B**), and 45 clusters representing different types of inhibitory neurons (*versus* 23 in mouse) (**Fig. 5B**). When compared with prior results from the human cortex, which characterized only eight transcriptomic cell types representing GABAergic neurons (Lake *et al.*, 2016), the targeted application of single nucleus sequencing demonstrated a significantly higher degree of GABAergic neuron complexity. This difference is likely due to a combination of improved sequencing techniques and increased sampling in a targeted anatomical domain enriched in GABAergic neurons.

Comparison of human molecular profiles with some profiles that define cortical cell types in mice (Tasic *et al.*, 2016; Lim *et al.*, 2018) revealed similarities but also differences (Hodge *et al.*, 2019). Almost all transcriptomic cell types in the human cortex showed homology with those in the mouse cortex. However, the expression level of certain genes within a homologous cell type varied greatly between species. Notably, genes encoding certain neurotransmitter molecule receptors (including serotonin receptors) showed the greatest divergence in expression between human and mouse. Moreover, the diversity of neurons in L1-4 was greater in the human cortex and almost all similar types of human excitatory neurons were found in more than one

layer (Hodge *et al.*, 2019). This distribution challenges the discrete laminar organization of cell types in the human cortex.

## 6. Correspondence across transcriptomic, anatomical, morphological, and physiological classification of mouse cortical neurons

Despite its major contribution toward cellular classification, single-cell transcriptomics cannot establish absolute boundaries between cell types on its own (**Figs. 4 and 5**). In addition, linking the transcriptomically defined cell types with the “classical” categories is challenging. Neuronal identification should require not only the unequivocal identification of the transcriptional landscape, but also the morphological, neurochemical, and electrophysiological properties, along with the synaptic partners (Tremblay, Lee and Rudy, 2016; Mihaljević *et al.*, 2019). Proposing a transcriptomic-based classification for a field traditionally centered on cellular anatomy, physiology and synaptic connectivity is challenging unless the classification strongly correlates with those features.

To inquire if the transcriptomic cell types found in the mouse cortex display specific anatomical and physiological properties, the same group analyzed the axonal projections and electrophysiological properties for a subset of transcriptomic types after their viral retrograde tracing or using different reporter Cre-lines for the selection of fluorescent cells ((Tasic *et al.*, 2016, 2017). RNA-seq analysis of retrograde-labeled neurons in mouse primary visual cortex shows different projections of transcriptionally defined excitatory subclasses. Retrograde-labeled cells from the ipsilateral thalamus were transcriptomically classified into L5b-Tph2, L5b-Cdh13, L5-Chrna6, L6a-Mgp and L6a-Sla types, which were validated as *Exc I* class neurons (CT). The retrograde-labeled cells from the contralateral VISp were transcriptomically classified into L5a-Batf3, L6a-Car12 and L6a-Syt17 cell types, which were validated as *Exc III* class neurons (IT).

In order to link transcriptomic types to the “classically” described inhibitory neurons, the authors also analyzed axonal projections and electrophysiology for a subset of transcriptomic types using transgenic mouse Cre-lines that allowed targeting specific cortical neurons based on their fluorescent expression of subclass markers (such as

1  
2  
3  
4  
5  
6  
7  
8  
9  
10  
11  
12  
13  
14  
15  
16  
17  
18  
19  
20  
21  
22  
23  
24  
25  
26  
27  
28  
29  
30  
31  
32  
33  
34  
35  
36  
37  
38  
39  
40  
41  
42  
43  
44  
45  
46  
47  
48  
49  
50  
51  
52  
53  
54  
55  
56  
57  
58  
59  
60

Nkx2.1, Reln and Ndnf) (Tasic *et al.*, 2016, 2017). They isolated cells from the upper layers of the *Nkx2.1*-CreERT2 line, which, when induced with tamoxifen perinatally, labels subsets of Pvalb and Sst neocortical interneurons. Computational analysis found that Pvalb-Cpne5 is enriched in the upper layers and may correspond to chandelier cells because it is the most transcriptionally distinct among the Pvalb types. Based on upper layer enrichment and Calb2 expression, the Sst-Cbln4 type most likely corresponds to previously characterized Calb2-positive Martinotti cells, which are enriched in the upper cortical layers. Transcriptomic analysis revealed an additional Calb2-positive Sst type, Sst-Chodl. Based on the expression of Npy, high levels of Nos and absence of Calb1, this type most likely corresponds to Nos expressing neurons, which are enriched in L5 and 6, and are likely long-range projecting neurons. The transcriptomically profiled neurons from the Cre line expressing Reln were classified into the two types likely corresponding to neurogliaform and single bouquet cells, which are highly enriched in L1.

The Patch-seq technique, which combines Patch-clamp physiology and scRNA-seq (Cadwell *et al.*, 2016; Lipovsek *et al.*, 2021) was used to investigate the correspondence of electrophysiological features with genome-wide expression signatures and transcriptomic cell type classification. Based on whole cell current clamp recordings of tdT+ cells from *Ndnf*-Cre line mice in L1 of VISp, the authors grouped cells into two categories: late-spiking (LS), and non-late spiking (NLS). LS neurons showed depolarizing ramp voltage near threshold, late spiking, and accelerating spike frequency. NLS neurons displayed the initial depolarizing response that was sufficient to induce an action potential at the onset of the current step in some trials. At slightly higher current intensities, all NLS neurons initiated a bout of late spiking after a period of quiescence. Reconstruction of two biocytin-filled, tdT+ neurons revealed one of them to have the tight, dense axonal arbor with small, bouton-like structures, and a relatively small dendritic tree that is typical of single bouquet neurons. The other neuron displayed axonal and dendritic arbors more similar to the recently described neurogliaform sparse-axon cells. Together, molecular, physiological and morphological analyses of L1 neurons labeled by the *Ndnf*-IRES2-dgCre line show that they correspond to neurogliaform cells. A strong correspondence between scRNA-seq, electrophysiology and morphology was shown for mouse neurogliaform cells in L1 (Tasic *et al.*, 2016, 2017).

The same team (Tasic *et al.*, 2017; Gouwens *et al.*, 2020) classify the neurons in the mouse visual cortex by combining morphological, electrophysiological and transcriptional features (Gouwens *et al.*, 2020). By using the Patch-seq technique in a highly standardized setting, Gouwens *et al.* created a database of 4,270 GABAergic interneurons with information on the electrical properties and transcriptomics of these neurons, as well as morphological data regarding 517 of these cells. These data allow for global understanding of the landscape of inhibitory cell types in the neocortex by combining distinct modalities at the single cell scale. The authors were able to draw boundaries among cell types by clustering sampled cells based on similarities in gene expression (T-types), morphology (M-types), and electrophysiology (E-types). The result is a consensus of morpho-electric-transcriptomic typing (MET-type), defining thirteen MET-types within the Sst-expressing cells, five within the Pvalb-expressing cells, two within the Lamp5 cells, three within the Sncg-expressing cells, and five within the Vip-expressing cells (Gouwens *et al.*, 2020).

In contrast with the limitations provided by using transcriptomics alone, this work allows mapping of historical data to a common naming scheme (Gouwens *et al.*, 2020), revealing substantial evidence for cross-modal correspondence in neocortical cell types and providing a complete roadmap for the mouse visual cortex. The authors pointed out several instances of previously defined cell types mapping to their consensus MET-type approach: e.g., the so-called L1 canopy cells map to Lamp5-MET-1 (Schuman *et al.*, 2019); the layer 2/3 and 5/6 fanning-out Martinotti cells map to the Sst-MET-3 and 4, respectively (Nigro, Hashikawa-Yamasaki and Rudy, 2018); and the translaminar fast-spiking cells map to Pvalb-MET-4 (Frandonig *et al.*, 2019). They also reveal new signatures of cortical inhibitory cell types such as clear soma depth profiles and axonal laminar innervation patterns. Sst MET-types, for instance, exhibit a cell type-specific preference for different cortical layers. By connecting data across modalities, the authors also observe a greater diversity of inhibitory neuron types than many previous studies. Mapping cell types across modalities and achieving consensus about inhibitory cortical types across labs is critical in order to comprehend the functional role of each cell type in cortical computations; however, the success of systematic annotation is still highly dependent on the cell type in question. For instance, it should be simple to map cell types across labs that are morphologically and transcriptomically unique and cluster tightly in these spaces (e.g., Sst/ Chodl and

1  
2  
3  
4  
5  
6  
7  
8  
9  
10  
11  
12  
13  
14  
15  
16  
17  
18  
19  
20  
21  
22  
23  
24  
25  
26  
27  
28  
29  
30  
31  
32  
33  
34  
35  
36  
37  
38  
39  
40  
41  
42  
43  
44  
45  
46  
47  
48  
49  
50  
51  
52  
53  
54  
55  
56  
57  
58  
59  
60

Chandelier cells). However, such a task might prove difficult for inhibitory classes that appear to exist on a genetic/functional continuum in which the functionally relevant boundaries are more difficult to define (e.g., Lamp5-MET-1 and Vip cells) (Gouwens *et al.*, 2020).

**7. Correspondence across transcriptomic, anatomical, morphological and physiological classification of human cortical neurons**

Some of the transcriptomic cell types in the human cortex fit well within the “classically” defined cell types, but others revealed previously unknown distinctions within broad neuronal classes. For example, the ‘rosehip’ cell, an inhibitory type neuron in L1 that has been described in the human cortex, but not in rodent one (Boldog *et al.*, 2018), showed high concordance between scRNA-seq, physiology and morphology. Rosehip cells are CCK-positive but cannabinoid receptor-negative, and they appear to selectively target distal dendrites of pyramidal neurons. Two interneuron types and two canonical pathways involving feed forward interneuron-to-interneuron connections were detected when high throughput electrophysiology capable of sampling all cell types was used to examine L1-situated inhibitory neurons in rodents (Lee *et al.*, 2015). Thus, the monosynaptic pyramidal cell preferring pathway initiated by rosehip cells does not appear to be a viable concept in the rodent L1 circuit. Furthermore, focal intra-layer inhibition restricted by the compact axonal arbor of rosehip cells to distal dendrites of a column of pyramidal cells is also missing from rodents. Similarly, the rosehip molecular signature appears to be very different from any previously published data from rodents. Many of the most selective genes associated with rosehip cells relate to synaptic structure and function, supporting the correspondence between transcriptional and anatomical phenotypes. Although the transcriptomic comparison was done between human temporal cortex and mouse visual cortex (Boldog *et al.*, 2018; Hodge *et al.*, 2019), regional differences seem unlikely to account for this difference, as anatomically defined rosehip cells were in multiple regions of human cortex. Rosehip cells may be of particular importance in compartmental control of back-propagating action potentials and their pairing with incoming excitatory inputs. Action potentials back-propagate to distal dendrites of human pyramidal cells and can be attenuated by rosehip cell activation. Thus, they may represent a mechanism for supplementary inhibitory control required to balance the potentially higher excitability

in human dendrites and might form the basis of spatially accurate modulation of interactions between long range excitatory inputs arriving to L1 and back-propagating action potentials. The rosehip cell clearly differs from neighboring neurogliaform cells and represents a type with highly distinctive transcriptomic signature, a highly distinctive morphological, physiological and connectional phenotype, and a strong correspondence between these properties.

A complete comparison of all cortical cell types and assessment of relative similarities between cell types should be possible in the future as more comprehensive transcriptome data become available and are being linked to other cellular phenotypes in multiple species.

## **8. Outlook toward defining the complete neuronal identity in the human cortex**

A remarkable contribution toward cataloging the variety of cell types in the mouse visual cortex and a clear validation for the transcriptomic cell types was provided by systematically combining single cell electrophysiology and transcriptomics (Gouwens *et al.*, 2020). It also emphasized the need for exercising caution when interpreting data acquired solely through genetic approaches. It is clear now that functionally relevant and distinct cell types require multiple parameters to be defined. This work also established a strong framework for the further classification of human cortical neurons, which will be useful in future functional studies. As a multimodal approach at the intersection of molecular neurobiology and physiology, Patch-seq is uniquely positioned to directly link gene expression to brain function. However, the journey toward achieving a universal classification system for cortical neurons is still underway. Ongoing work in the Allen Institute for Brain Science has been examining additional parameters such as connectivity, gene expression during development, and *in vivo* activity. The details of cellular and subcellular connectivity that electron microscopy brings to the cell type classification system are particularly intriguing. Experimental tools, such as novel spatial transcriptomic methods, are becoming more available to aid in phenotypic characterization of transcriptionally defined cell types in

1  
2  
3  
4  
5  
6  
7  
8  
9  
10  
11  
12  
13  
14  
15  
16  
17  
18  
19  
20  
21  
22  
23  
24  
25  
26  
27  
28  
29  
30  
31  
32  
33  
34  
35  
36  
37  
38  
39  
40  
41  
42  
43  
44  
45  
46  
47  
48  
49  
50  
51  
52  
53  
54  
55  
56  
57  
58  
59  
60

model animals and even humans (Wang *et al.*, 2004; Battich, Stoeger and Pelkmans, 2013; Lein, Borm and Linnarsson, 2017; Gyllborg *et al.*, 2020; Qian *et al.*, 2020). A logical next step is to map back such expression patterns *in situ* within developing tissues and/or mature organs. However, spatial transcriptomic analysis in human adult tissue presents a particular scaling challenge. To help in this direction, a spatial transcriptomic-related platforms called the large-area spatial transcriptomic (LaST) map and has provided a pipeline for mapping quantitative gene expression in single cells across vast mouse and human tissue areas (Bayraktar *et al.*, 2020). The LaST map demonstrated reproducibility across multiple tissue samples/sections and should be adaptable for a range of other tissues to obtain regional/qualitative and cellular/quantitative information from ISH reintegrated into 2D tissue maps, including the human cortex.

While major consortium efforts (such as SpaceTx consortium) generate the transcriptomic framework, linking different types of data to it will likely be most effective as a distributed community effort. On this line and as part of the Human Cell Atlas, Langseth *et al* (2021) utilized the predefined taxonomy of cells to create maps of histological tissue structures of the human temporal lobe (Langseth *et al.*, 2021). The mapped the cortical cell types previously classified by snRNA-seq (Hodge *et al.*, 2019), were combined with *in situ* sequencing gene expression *via* probabilistic cell typing (Gyllborg *et al.*, 2020; Qian *et al.*, 2020; Marco Salas *et al.*, 2021). The resulted cortical cell types were found to be arranged in layers, but less layer-restricted than expected, advocating that anatomical location alone is not sufficient to characterize a cell and the layer boundaries are not sharp in the human cortex. In addition, some classical markers, such as *SST*, were not prioritized by the gene selection approach; therefore, subclass genes were used for cell calls. By using this approach, even rare cell types, such as the *SST + CHODL + cell type* (Inh L3-6 *SST NPY*), could be typed. This combinatorial detection approach allowed the precise assignment of molecularly defined cell classes as well as their subtypes *in situ*.

In functional investigations, it is still common practice to use single Cre lines to define a cell type, which is not possible for the human cortex *in vivo*. The new development of human brain cortical tissue derived from pluripotent stem cells, such as brain organoids, cortical organoids and cortical “assembloids” (Amin and Paşca, 2018; Arlotta and Paşca, 2019), combined with human reporter lines, could shed light on



early stages of corticogenesis to neuronal network formation and also provide help in functional studies, such as by using Patch-seq (Cadwell *et al.*, 2016; Lipovsek *et al.*, 2021), even though the maturation level of human neurons generated *in vitro* with the current methods is still far from that of adult brain tissue.

Optimal classification of human cortical neuronal subtypes, like that of other species, should involve a greater understanding of their origins and trajectories during development and maturation. Several recent studies have focused on human cell types during brain development and have started to provide human-specific features, such as different progenitor cell types in the dorsal telencephalic SVZ (Hansen *et al.*, 2010; Betizeau *et al.*, 2013), persistence of CRC cells in the adult human neocortex (Belichenko *et al.*, 1995) but also single-cell transcriptional maps during primate development (Bakken *et al.*, 2016).

Together, these approaches provide convergent evidence for a robust description of cell type identity as well as multiple lines of evidence for species conservation or divergent aspects, in which neurodevelopment plays a key part.

Convergent transcriptomic, anatomical and functional research in the human cortex holds a lot of promise for determining which features are conserved and which are divergent among mammals. Defining the identity and function of neurons that are specific or enriched in human cortical circuits could be important in understanding pathological alterations. A better understanding of human cellular content and circuit organization in the cerebral cortex could help to overcome the current lack of success in translating promising results in rodents to effective treatment against human neurologic and neuropsychiatric disorders (Gao and Penzes, 2015; Velmeshev *et al.*, 2019).

## References

Abdelaal, T. *et al.* (2019) 'A comparison of automatic cell identification methods for single-cell RNA sequencing data', *Genome Biology*, 20(1). doi: 10.1186/s13059-019-1795-z.

- Amin, N. D. and Paşca, S. P. (2018) 'Building Models of Brain Disorders with Three-Dimensional Organoids', *Neuron*. Cell Press, pp. 389–405. doi: 10.1016/j.neuron.2018.10.007.
- Amunts, K. and Zilles, K. (2015) 'Architectonic Mapping of the Human Brain beyond Brodmann', *Neuron*. Cell Press, pp. 1086–1107. doi: 10.1016/j.neuron.2015.12.001.
- Arlotta, P. and Paşca, S. P. (2019) 'Cell diversity in the human cerebral cortex: from the embryo to brain organoids', *Current Opinion in Neurobiology*. Elsevier Ltd, pp. 194–198. doi: 10.1016/j.conb.2019.03.001.
- Azevedo, F. A. C. *et al.* (2009) 'Equal numbers of neuronal and nonneuronal cells make the human brain an isometrically scaled-up primate brain', *Journal of Comparative Neurology*, 513(5), pp. 532–541. doi: 10.1002/cne.21974.
- Baker, A. *et al.* (2018) 'Specialized subpopulations of deep-layer pyramidal neurons in the neocortex: Bridging cellular properties to functional consequences', *Journal of Neuroscience*, 38(24), pp. 5441–5455. doi: 10.1523/JNEUROSCI.0150-18.2018.
- Bakken, T. *et al.* (2017) 'Cell type discovery and representation in the era of high-content single cell phenotyping', *BMC Bioinformatics*, 18. doi: 10.1186/s12859-017-1977-1.
- Bakken, T. E. *et al.* (2016) 'A comprehensive transcriptional map of primate brain development', *Nature*, 535(7612), pp. 367–375. doi: 10.1038/nature18637.
- Bakken, T. E. *et al.* (2018) 'Single-nucleus and single-cell transcriptomes compared in matched cortical cell types', *PLoS ONE*, 13(12). doi: 10.1371/journal.pone.0209648.
- Battich, N., Stoeger, T. and Pelkmans, L. (2013) 'Image-based transcriptomics in thousands of single human cells at single-molecule resolution', *Nature Methods*, 10(11), pp. 1127–1136. doi: 10.1038/nmeth.2657.
- Bayraktar, O. A. *et al.* (2020) 'Astrocyte layers in the mammalian cerebral cortex revealed by a single-cell in situ transcriptomic map', *Nature Neuroscience*, 23(4), pp. 500–509. doi: 10.1038/s41593-020-0602-1.
- Belichenko, P. V. *et al.* (1995) 'Calretinin-positive cajal-retzius cells persist in the adult human neocortex', *NeuroReport*, 6(14), pp. 1869–1874. doi:

10.1097/00001756-199510020-00012.

Betizeau, M. *et al.* (2013) 'Precursor Diversity and Complexity of Lineage Relationships in the Outer Subventricular Zone of the Primate', *Neuron*, 80(2), pp. 442–457. doi: 10.1016/j.neuron.2013.09.032.

Boldog, E. *et al.* (2018) 'Transcriptomic and morphophysiological evidence for a specialized human cortical GABAergic cell type', *Nature Neuroscience*, 21(9), pp. 1185–1195. doi: 10.1038/s41593-018-0205-2.

Bortone, D. S., Olsen, S. R. and Scanziani, M. (2014) 'Translaminar inhibitory cells recruited by layer 6 corticothalamic neurons suppress visual cortex', *Neuron*, 82(2), pp. 474–485. doi: 10.1016/j.neuron.2014.02.021.

*Brain Map* - *brain-map.org* (no date).

Butler, A. *et al.* (2018) 'Integrating single-cell transcriptomic data across different conditions, technologies, and species', *Nature Biotechnology*, 36(5), pp. 411–420. doi: 10.1038/nbt.4096.

Cadwell, C. R. *et al.* (2016) 'Electrophysiological, transcriptomic and morphologic profiling of single neurons using Patch-seq', *Nature Biotechnology*, 34(2), pp. 199–203. doi: 10.1038/nbt.3445.

Cadwell, C. R. *et al.* (2019) 'Development and Arealization of the Cerebral Cortex', *Neuron*. Cell Press, pp. 980–1004. doi: 10.1016/j.neuron.2019.07.009.

Darmanis, S. *et al.* (2015) 'A survey of human brain transcriptome diversity at the single cell level', *Proceedings of the National Academy of Sciences of the United States of America*, 112(23), pp. 7285–7290. doi: 10.1073/pnas.1507125112.

DeFelipe, J. (2011) 'The evolution of the brain, the human nature of cortical circuits, and intellectual creativity', *Frontiers in Neuroanatomy*. doi: 10.3389/fnana.2011.00029.

Ecker, J. R. *et al.* (2017) 'The BRAIN Initiative Cell Census Consortium: Lessons Learned toward Generating a Comprehensive Brain Cell Atlas', *Neuron*. Cell Press, pp. 542–557. doi: 10.1016/j.neuron.2017.10.007.

Eyal, G. *et al.* (2016) 'Unique membrane properties and enhanced signal processing

in human neocortical neurons', *eLife*, 5(OCTOBER2016). doi: 10.7554/eLife.16553.

Finlay, B. L. and Darlington, R. B. (1995) 'Linked regularities in the development and evolution of mammalian brains', *Science*, 268(5217), pp. 1578–1584. doi: 10.1126/science.7777856.

Frandonig, J. E. *et al.* (2019) 'The Synaptic Organization of Layer 6 Circuits Reveals Inhibition as a Major Output of a Neocortical Sublamina', *Cell Reports*, 28(12), pp. 3131–3143.e5. doi: 10.1016/j.celrep.2019.08.048.

Froudarakis, E. *et al.* (2019) 'The Visual Cortex in Context', *Annual Review of Vision Science*. Annual Reviews Inc., pp. 317–339. doi: 10.1146/annurev-vision-091517-034407.

Gao, R. and Penzes, P. (2015) 'Common Mechanisms of Excitatory and Inhibitory Imbalance in Schizophrenia and Autism Spectrum Disorders', *Current Molecular Medicine*, 15(2), pp. 146–167. doi: 10.2174/1566524015666150303003028.

García-Cabezas, M. A., Hacker, J. L. and Zikopoulos, B. (2020) 'A Protocol for Cortical Type Analysis of the Human Neocortex Applied on Histological Samples, the Atlas of Von Economo and Koskinas, and Magnetic Resonance Imaging', *Frontiers in Neuroanatomy*, 14. doi: 10.3389/fnana.2020.576015.

Glezer, I., Bittencourt, J. C. and Rivest, S. (2009) 'Neuronal expression of Cd36, Cd44, and Cd83 antigen transcripts maps to distinct and specific murine brain circuits', *Journal of Comparative Neurology*, 517(6), pp. 906–924. doi: 10.1002/cne.22185.

Gouwens, N. W. *et al.* (2020) 'Integrated Morphoelectric and Transcriptomic Classification of Cortical GABAergic Cells', *Cell*, 183(4), pp. 935–953.e19. doi: 10.1016/j.cell.2020.09.057.

Greig, L. C. *et al.* (2013) 'Molecular logic of neocortical projection neuron specification, development and diversity', *Nature Reviews Neuroscience*, pp. 755–769. doi: 10.1038/nrn3586.

Gyllborg, D. *et al.* (2020) 'Hybridization-based in situ sequencing (HybISS) for spatially resolved transcriptomics in human and mouse brain tissue', *Nucleic Acids Research*, 48(19), pp. e112–e112. doi: 10.1093/nar/gkaa792.

- Habib, N. *et al.* (2017) 'Massively parallel single-nucleus RNA-seq with DroNc-seq', *Nature Methods*, 14(10), pp. 955–958. doi: 10.1038/nmeth.4407.
- Hansen, D. V. *et al.* (2010) 'Neurogenic radial glia in the outer subventricular zone of human neocortex', *Nature*, 464(7288), pp. 554–561. doi: 10.1038/nature08845.
- Hansen, D. V. *et al.* (2013) 'Non-epithelial stem cells and cortical interneuron production in the human ganglionic eminences', *Nature Neuroscience*, 16(11), pp. 1576–1587. doi: 10.1038/nn.3541.
- Harris, K. D. and Shepherd, G. M. G. (2015) 'The neocortical circuit: Themes and variations', *Nature Neuroscience*. Nature Publishing Group, pp. 170–181. doi: 10.1038/nn.3917.
- Hawrylycz, M. *et al.* (2015) 'Canonical genetic signatures of the adult human brain', *Nature Neuroscience*, 18(12), pp. 1832–1844. doi: 10.1038/nn.4171.
- Hébert, J. M. and Fishell, G. (2008) 'The genetics of early telencephalon patterning: Some assembly required', *Nature Reviews Neuroscience*, pp. 678–685. doi: 10.1038/nrn2463.
- Herculano-Houzel, S., Mota, B. and Lent, R. (2006) 'Cellular scaling rules for rodent brains', *Proceedings of the National Academy of Sciences of the United States of America*, 103(32), pp. 12138–12143. doi: 10.1073/pnas.0604911103.
- Hill, R. S. and Walsh, C. A. (2005) 'Molecular insights into human brain evolution', *Nature*. Nature Publishing Group, pp. 64–67. doi: 10.1038/nature04103.
- Hladnik, A. *et al.* (2014) 'Spatio-temporal extension in site of origin for cortical calretinin neurons in primates', *Frontiers in Neuroanatomy*, 8(JUN). doi: 10.3389/fnana.2014.00050.
- Hodge, R. D. *et al.* (2019) 'Conserved cell types with divergent features in human versus mouse cortex', *Nature*, 573(7772), pp. 61–68. doi: 10.1038/s41586-019-1506-7.
- Johnson, M. B. and Walsh, C. A. (2017) 'Cerebral cortical neuron diversity and development at single-cell resolution', *Current Opinion in Neurobiology*. Elsevier Ltd, pp. 9–16. doi: 10.1016/j.conb.2016.11.001.

Kang, H. J. *et al.* (2011) 'Spatio-temporal transcriptome of the human brain', *Nature*, 478(7370), pp. 483–489. doi: 10.1038/nature10523.

Kiselev, V. Y., Andrews, T. S. and Hemberg, M. (2019) 'Challenges in unsupervised clustering of single-cell RNA-seq data', *Nature Reviews Genetics*. Nature Publishing Group, pp. 273–282. doi: 10.1038/s41576-018-0088-9.

Kostović, I., Judaš, M. and Sedmak, G. (2011) 'Developmental history of the subplate zone, subplate neurons and interstitial white matter neurons: Relevance for schizophrenia', *International Journal of Developmental Neuroscience*, 29(3), pp. 193–205. doi: 10.1016/j.ijdevneu.2010.09.005.

Kriegstein, A., Noctor, S. and Martínez-Cerdeño, V. (2006) 'Patterns of neural stem and progenitor cell division may underlie evolutionary cortical expansion', *Nature Reviews Neuroscience*, pp. 883–890. doi: 10.1038/nrn2008.

Krishnaswami, S. R. *et al.* (2016) 'Using single nuclei for RNA-seq to capture the transcriptome of postmortem neurons', *Nature Protocols*, 11(3), pp. 499–524. doi: 10.1038/nprot.2016.015.

Kwan, K. Y., Šestan, N. and Anton, E. S. (2012) 'Transcriptional co-regulation of neuronal migration and laminar identity in the neocortex', *Development*, pp. 1535–1546. doi: 10.1242/dev.069963.

Lake, B. B. *et al.* (2016) 'Neuronal subtypes and diversity revealed by single-nucleus RNA sequencing of the human brain', *Science*, 352(6293), pp. 1586–1590. doi: 10.1126/science.aaf1204.

Lake, B. B. *et al.* (2017) 'A comparative strategy for single-nucleus and single-cell transcriptomes confirms accuracy in predicted cell-type expression from nuclear RNA', *Scientific Reports*, 7(1). doi: 10.1038/s41598-017-04426-w.

Lake, B. B. *et al.* (2018) 'Integrative single-cell analysis of transcriptional and epigenetic states in the human adult brain', *Nature Biotechnology*, 36(1), pp. 70–80. doi: 10.1038/nbt.4038.

Langseth, C. M. *et al.* (2021) 'Comprehensive in situ mapping of human cortical transcriptomic cell types', *Communications Biology*, 4(1), p. 998. doi: 10.1038/s42003-021-02517-z.



1  
2  
3 Lee, A. J. *et al.* (2015) 'Canonical Organization of Layer 1 Neuron-Led Cortical  
4 Inhibitory and Disinhibitory Interneuronal Circuits', *Cerebral Cortex*, 25(8), pp. 2114–  
5 2126. doi: 10.1093/cercor/bhu020.  
6  
7

8  
9 Lein, E., Borm, L. E. and Linnarsson, S. (2017) 'The promise of spatial  
10 transcriptomics for neuroscience in the era of molecular cell typing', *Science*.  
11 American Association for the Advancement of Science, pp. 64–69. doi:  
12 10.1126/science.aan6827.  
13  
14

15  
16 Lein, E. S. *et al.* (2007) 'Genome-wide atlas of gene expression in the adult mouse  
17 brain', *Nature*, 445(7124), pp. 168–176. doi: 10.1038/nature05453.  
18  
19

20  
21 Lent, R. *et al.* (2012) 'How many neurons do you have? Some dogmas of  
22 quantitative neuroscience under revision', *European Journal of Neuroscience*, pp. 1–  
23 9. doi: 10.1111/j.1460-9568.2011.07923.x.  
24  
25

26  
27 Li, H. *et al.* (2017) 'Reference component analysis of single-cell transcriptomes  
28 elucidates cellular heterogeneity in human colorectal tumors', *Nature Genetics*,  
29 49(5), pp. 708–718. doi: 10.1038/ng.3818.  
30  
31

32  
33 Lim, L. *et al.* (2018) 'Development and Functional Diversification of Cortical  
34 Interneurons', *Neuron*. Cell Press, pp. 294–313. doi: 10.1016/j.neuron.2018.10.009.  
35  
36

37  
38 Lipovsek, M. *et al.* (2021) 'Patch-seq: Past, present, and future', in *Journal of*  
39 *Neuroscience*. Society for Neuroscience, pp. 937–946. doi:  
40 10.1523/JNEUROSCI.1653-20.2020.  
41  
42

43  
44 Lodato, S. and Arlotta, P. (2015) 'Generating Neuronal Diversity in the Mammalian  
45 Cerebral Cortex', *Annual Review of Cell and Developmental Biology*, 31, pp. 699–  
46 720. doi: 10.1146/annurev-cellbio-100814-125353.  
47  
48

49  
50 Lui, J. H., Hansen, D. V. and Kriegstein, A. R. (2011) 'Development and evolution of  
51 the human neocortex', *Cell*. Elsevier B.V., pp. 18–36. doi:  
52 10.1016/j.cell.2011.06.030.  
53  
54

55  
56 La Manno, G. *et al.* (2021) 'Molecular architecture of the developing mouse brain',  
57 *Nature*, 596(7870), pp. 92–96. doi: 10.1038/s41586-021-03775-x.  
58  
59

60  
Marco Salas, S. *et al.* (2021) 'Matisse: a MATLAB-based analysis toolbox for in situ  
sequencing expression maps', *BMC Bioinformatics*, 22(1), p. 391. doi:



10.1186/s12859-021-04302-5.

Mihaljević, B. *et al.* (2019) 'Classification of GABAergic interneurons by leading neuroscientists', *Scientific Data*, 6(1). doi: 10.1038/s41597-019-0246-8.

Moffitt, J. R. *et al.* (2016) 'High-performance multiplexed fluorescence in situ hybridization in culture and tissue with matrix imprinting and clearing', *Proceedings of the National Academy of Sciences of the United States of America*, 113(50), pp. 14456–14461. doi: 10.1073/pnas.1617699113.

Molnár, Z. and Clowry, G. (2012) 'Cerebral cortical development in rodents and primates', in *Progress in Brain Research*. Elsevier B.V., pp. 45–70. doi: 10.1016/B978-0-444-53860-4.00003-9.

Nigro, M. J., Hashikawa-Yamasaki, Y. and Rudy, B. (2018) 'Diversity and connectivity of layer 5 somatostatin-expressing interneurons in the mouse barrel cortex', *Journal of Neuroscience*, 38(7), pp. 1622–1633. doi: 10.1523/JNEUROSCI.2415-17.2017.

Qian, X. *et al.* (2020) 'Probabilistic cell typing enables fine mapping of closely related cell types in situ', *Nature Methods*, 17(1), pp. 101–106. doi: 10.1038/s41592-019-0631-4.

Raghanti, M. A. *et al.* (2013) 'Neuropeptide Y-immunoreactive Neurons in the Cerebral Cortex of Humans and Other Haplorrhine Primates', *American Journal of Primatology*, 75(5), pp. 415–424. doi: 10.1002/ajp.22082.

Ranjan, B. *et al.* (2021) 'scConsensus: combining supervised and unsupervised clustering for cell type identification in single-cell RNA sequencing data', *BMC Bioinformatics*, 22(1). doi: 10.1186/s12859-021-04028-4.

Regev, A. *et al.* (2017) 'The human cell atlas', *eLife*, 6. doi: 10.7554/eLife.27041.

Schuman, B. *et al.* (2019) 'Four unique interneuron populations reside in neocortical layer 1', *Journal of Neuroscience*, 39(1), pp. 125–139. doi: 10.1523/JNEUROSCI.1613-18.2018.

Shen, Q. *et al.* (2006) 'The timing of cortical neurogenesis is encoded within lineages of individual progenitor cells', *Nature Neuroscience*, 9(6), pp. 743–751. doi: 10.1038/nn1694.

- Staiger, J. F. *et al.* (2004) 'Functional diversity of layer IV spiny neurons in rat somatosensory cortex: Quantitative morphology of electrophysiologically characterized and biocytin labeled cells', *Cerebral Cortex*, 14(6), pp. 690–701. doi: 10.1093/cercor/bhh029.
- Tang, F. *et al.* (2009) 'mRNA-Seq whole-transcriptome analysis of a single cell', *Nature Methods*, 6(5), pp. 377–382. doi: 10.1038/nmeth.1315.
- Tasic, B. *et al.* (2016) 'Adult mouse cortical cell taxonomy revealed by single cell transcriptomics', *Nature Neuroscience*, 19(2), pp. 335–346. doi: 10.1038/nn.4216.
- Tasic, B. *et al.* (2017) 'Shared and distinct transcriptomic cell types across neocortical areas', *bioRxiv*, p. 229542. doi: 10.1101/229542.
- Tremblay, R., Lee, S. and Rudy, B. (2016) 'GABAergic Interneurons in the Neocortex: From Cellular Properties to Circuits', *Neuron*. Cell Press, pp. 260–292. doi: 10.1016/j.neuron.2016.06.033.
- Turrero García, M. and Harwell, C. C. (2017) 'Radial glia in the ventral telencephalon', *FEBS Letters*. Wiley Blackwell, pp. 3942–3959. doi: 10.1002/1873-3468.12829.
- Velmeshev, D. *et al.* (2019) 'Single-cell genomics identifies cell type-specific molecular changes in autism', *Science*, 364(6441), pp. 685–689. doi: 10.1126/science.aav8130.
- Wagstyl, K. *et al.* (2020) 'BigBrain 3D atlas of cortical layers: Cortical and laminar thickness gradients diverge in sensory and motor cortices', *PLoS Biology*, 18(4). doi: 10.1371/journal.pbio.3000678.
- Wang, X. *et al.* (2018) 'Three-dimensional intact-tissue sequencing of single-cell transcriptional states', *Science*, 361(6400). doi: 10.1126/science.aat5691.
- Wang, Y. *et al.* (2004) 'Anatomical, physiological and molecular properties of Martinotti cells in the somatosensory cortex of the juvenile rat', *Journal of Physiology*, 561(1), pp. 65–90. doi: 10.1113/jphysiol.2004.073353.
- Wonders, C. P. and Anderson, S. A. (2006) 'The origin and specification of cortical interneurons', *Nature Reviews Neuroscience*, pp. 687–696. doi: 10.1038/nrn1954.

1  
2  
3  
4  
5  
6  
7  
8  
9  
10  
11  
12  
13  
14  
15  
16  
17  
18  
19  
20  
21  
22  
23  
24  
25  
26  
27  
28  
29  
30  
31  
32  
33  
34  
35  
36  
37  
38  
39  
40  
41  
42  
43  
44  
45  
46  
47  
48  
49  
50  
51  
52  
53  
54  
55  
56  
57  
58  
59  
60

Woodruff, A. R., Anderson, S. A. and Yuste, R. (2010) ‘The enigmatic function of chandelier cells’, *Frontiers in Neuroscience*. Frontiers, p. 201. doi: 10.3389/fnins.2010.00201.

Xu, X., Roby, K. D. and Callaway, E. M. (2010) ‘Immunochemical characterization of inhibitory mouse cortical neurons: Three chemically distinct classes of inhibitory cells’, *Journal of Comparative Neurology*, 518(3), pp. 389–404. doi: 10.1002/cne.22229.

Yuste, R. *et al.* (2020) ‘A community-based transcriptomics classification and nomenclature of neocortical cell types’, *Nature Neuroscience*. Nature Research, pp. 1456–1468. doi: 10.1038/s41593-020-0685-8.

Zeisel, A. *et al.* (2015) ‘Cell types in the mouse cortex and hippocampus revealed by single-cell RNA-seq’, *Science*, 347(6226), pp. 1138–1142. doi: 10.1126/science.aaa1934.

Zhao, Y. *et al.* (2008) ‘Distinct molecular pathways of development of telencephalic interneuron subtypes revealed through analysis of Lhx6 mutants’, *Journal of Comparative Neurology*, 510(1), pp. 79–99. doi: 10.1002/cne.21772.

# Figure legends:

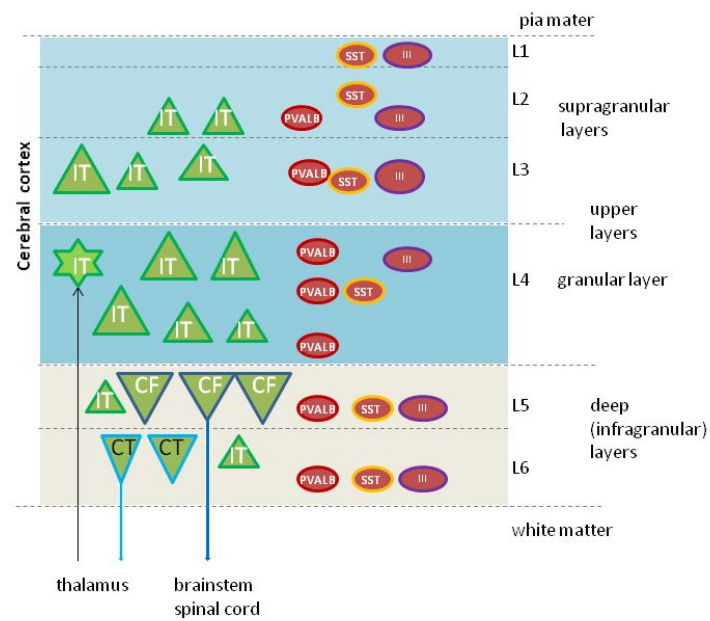


**Figure 1. Schematic representation of the mammalian cerebral cortex**

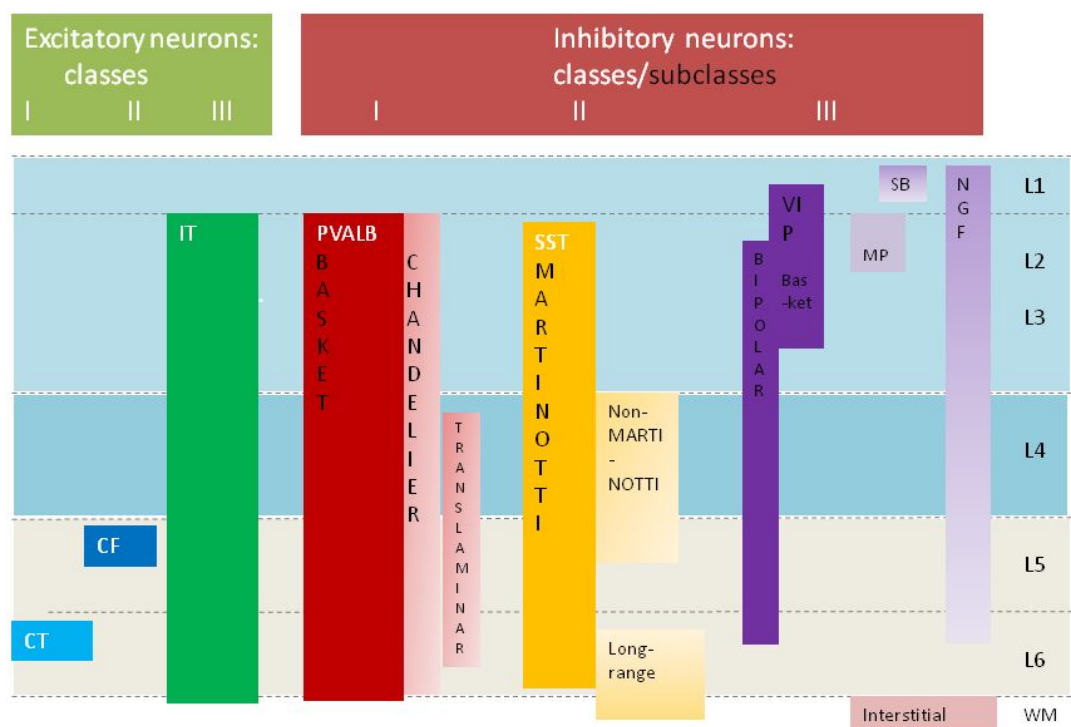


**Figure 2. Classical clasification of the cortical neurons and the localatization of the main classes and subclasses.** CT cortico-thalamic, CF cortico-fugal, IT intratelencephalic, PVALB parvalbumin, SST somatostatin, VIP vasoactive intestinal peptide, MP multipolar, SB single bouquet, NGF neurogliaform, WM white matter.

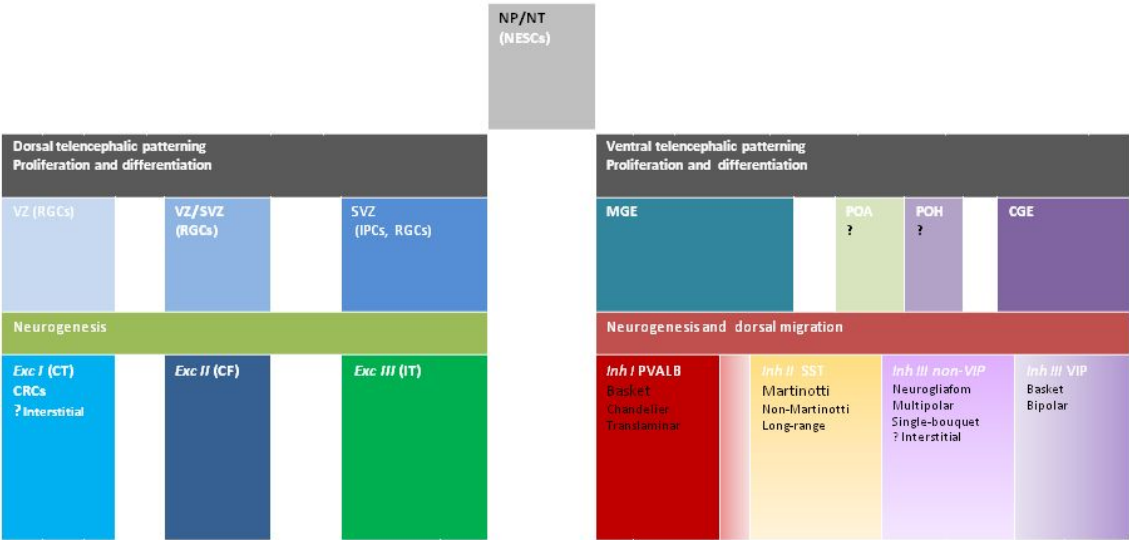


**Figure 3. Progenitors and developmental pathways of the cortical neurons**

NP neural plate, NT neural tube, NESCs neuroepithelial stem cells, VZ ventricular zone, SVZ subventricular zone, RGCs radial glial cells, IPCs intermediate progenitor cells, CRCs Cajal-Retzius cells, MGE medial ganglionic eminence, CGE caudal ganglionic eminence, POA preoptic area, POH preoptic-hypothalamic region, CT cortico-thalamic, CF cortico-fugal, IT intratelencephalic, PVALB parvalbumin, SST somatostatin, VIP vasoactive intestinal peptide.

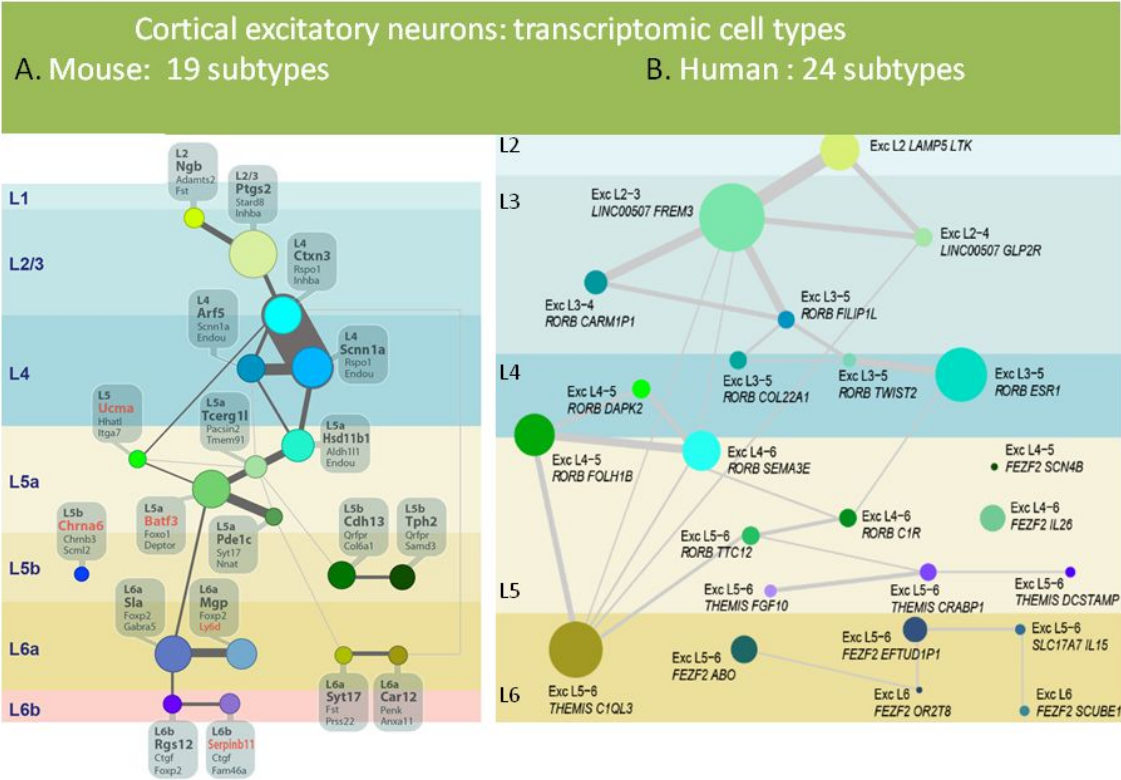


**Figure 4. Transcriptomic types of mouse (A) and human (B) excitatory cortical neurons** (adapted from Tasic *et al.*, 2016, 2017 (A) and Hodge *et al.*, 2019 (B))



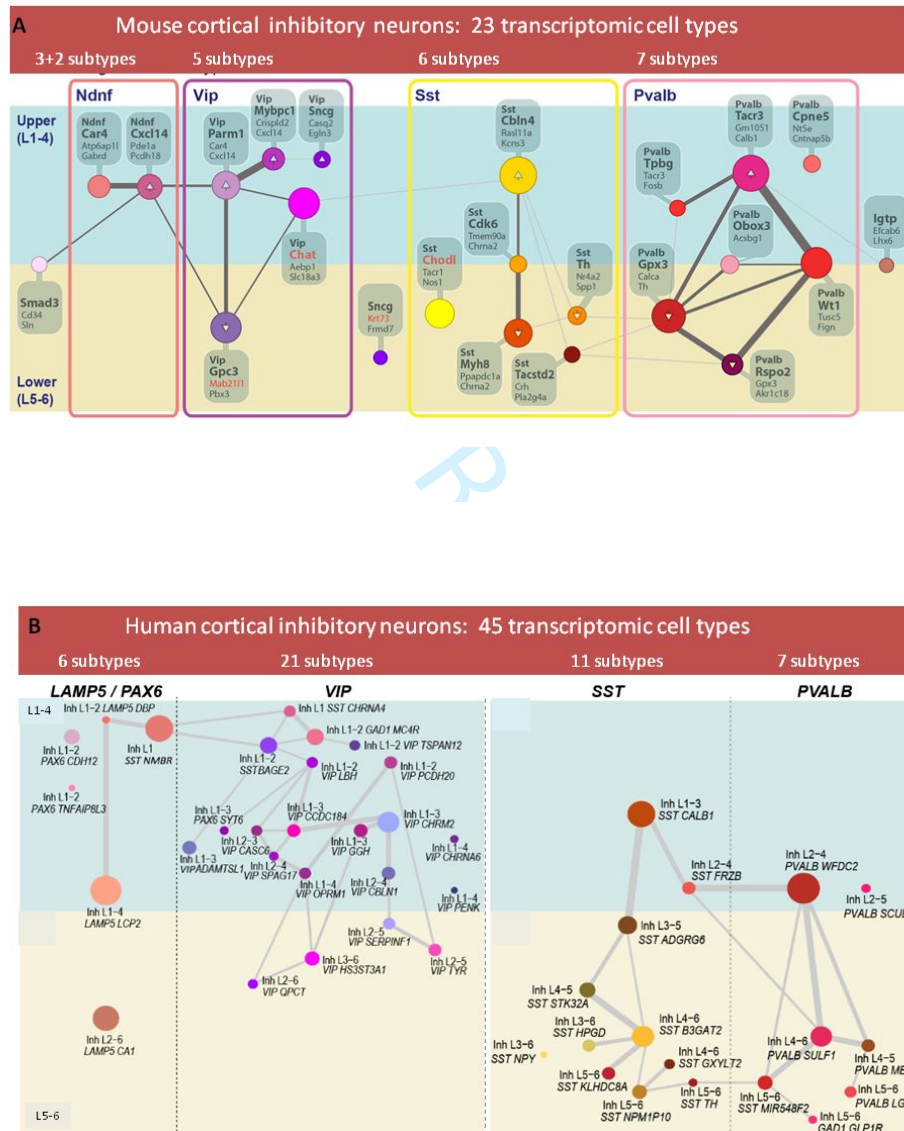


**Figure 5. Transcriptomic types of mouse (A) and human (B) inhibitory cortical neurons** (adapted from Tasic *et al.*, 2016, 2017 (A) and Hodge *et al.*, 2019 (B))

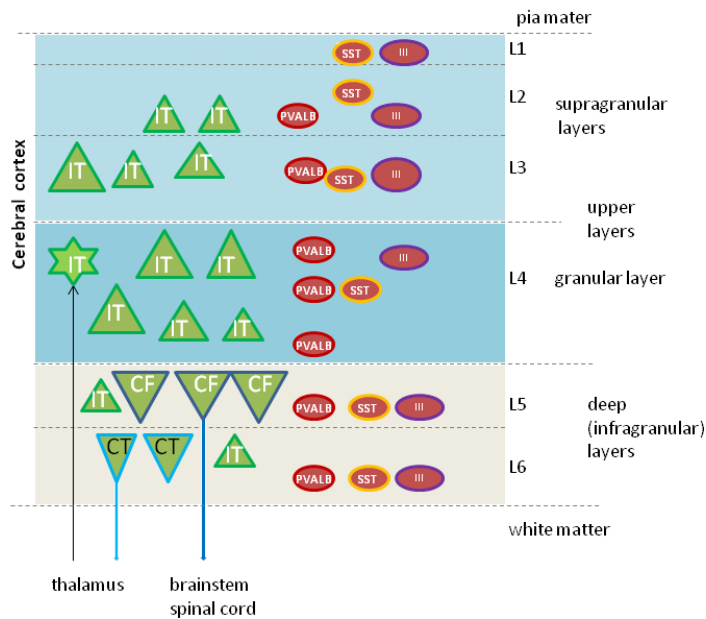


Figure 1. Schematic representation of the mammalian cerebral cortex

254x190mm (96 x 96 DPI)

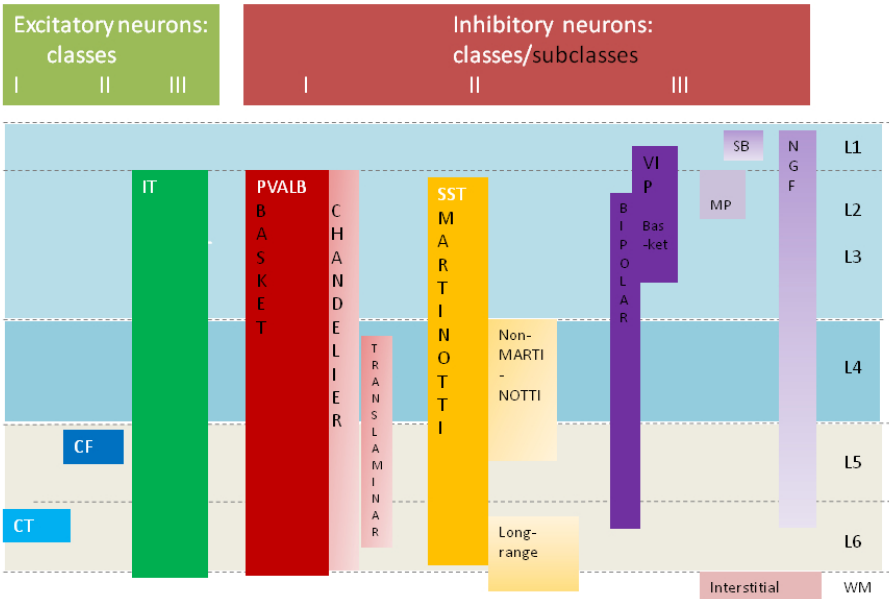


Figure 2. Classical clasification of the cortical neurons and the locatization of the main classes and subclasses. CT cortico-thalamic, CF cortico-fugal, IT intratelencephalic, PVALB parvalbumin, SST somatostatin, VIP vasoactive intestinal peptide, MP multipolar, SB single bouquet, NGF neurogliaform, WM white matter.

254x190mm (96 x 96 DPI)

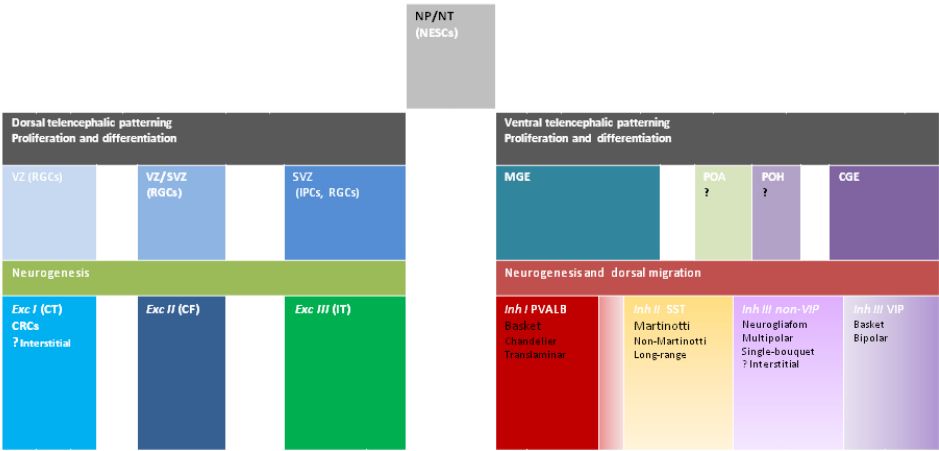


Figure 3. Progenitors and developmental pathways of the cortical neurons  
NP neural plate, NT neural tube, NESCs neuroepithelial stem cells, VZ ventricular zone, SVZ subventricular zone, RGCs radial glial cells, IPCs intermediate progenitor cells, CRCs Cajal-Retzius cells, MGE medial ganglionic eminence, CGE caudal ganglionic eminence, POA preoptic area, POH preoptic-hypothalamic region, CT cortico-thalamic, CF cortico-fugal, IT intratelencephalic, PVALB parvalbumin, SST somatostatin, VIP vasoactive intestinal peptide.

254x190mm (96 x 96 DPI)

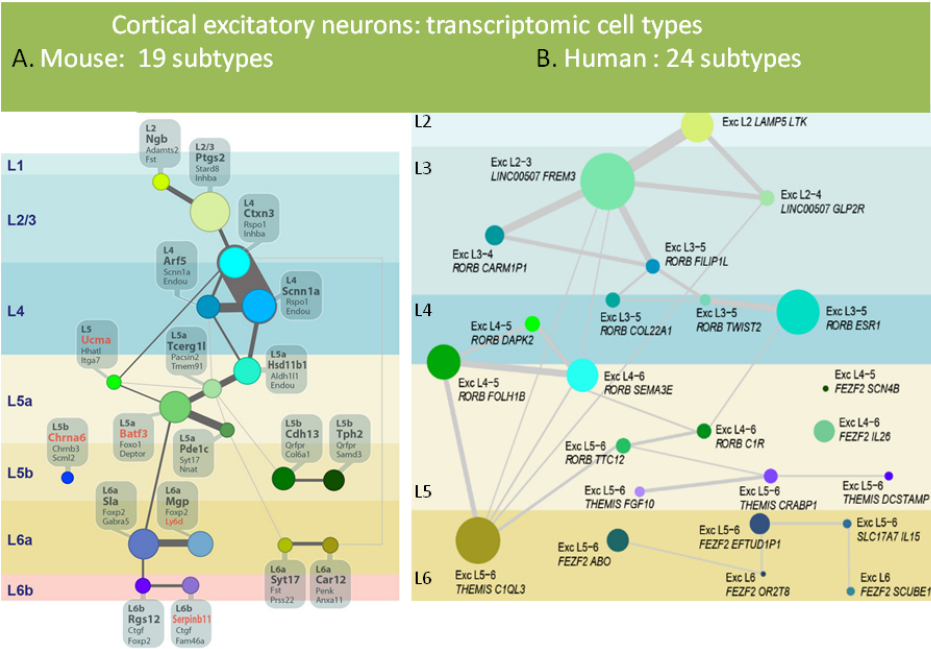
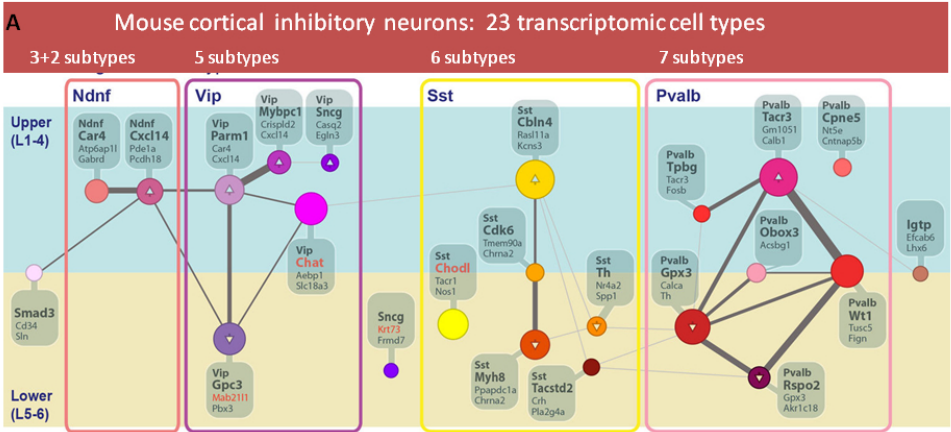


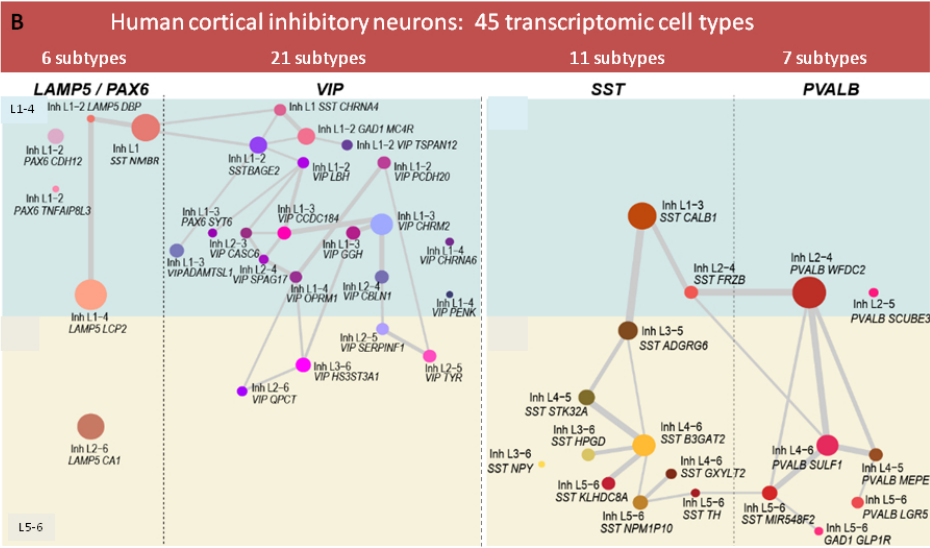
Figure 4. Transcriptomic types of mouse (A) and human (B) excitatory cortical neurons (adapted from Tasic et al., 2016 (A) and Hodge et al., 2019 (B))

254x190mm (96 x 96 DPI)



254x190mm (96 x 96 DPI)





254x190mm (96 x 96 DPI)